

Induction of DNA-Double-Strand Breaks by Auger Electrons from ^{99m}Tc Complexes with DNA-Binding Ligands

Pascal Häfliger,^[a] Nikos Agorastos,^[a] Bernhard Spingler,^[a] Oleg Georgiev,^[b] Giampietro Viola,^[c] and Roger Alberto^{*[a]}

The potential of certain Auger electron emitting nuclides for systemic radiotherapeutic applications has recently gained much attention. In particular, the ability of several nuclides, including ^{111}In , ^{125}I , and ^{123}I , to induce DNA double-strand breaks (dsb), a good indicator of cytotoxicity, has been extensively studied. However, this ability has never previously been shown experimentally for ^{99m}Tc , which, besides the well-known γ radiation that is used for diagnostic applications, also emits an average of 1.1 conversion electrons and 4 Auger or Coster–Kronig electrons per decay. Owing to the short range of Auger electrons, the radionuclide needs to be located very close to the DNA for dsb to occur. We synthesized two cationic ^{99m}Tc -tricarbyl complexes with pendant DNA binders, pyrene and anthraquinone. The X-ray crys-

tal structures of the two complexes could be elucidated. Linear dichroism and UV/Vis spectroscopy revealed that the complex with pyrene intercalates DNA with a stability constant, K , of $1.1 \times 10^6 \text{ M}^{-1}$, while the analogous complex with anthraquinone interacts with DNA in a groove-binding mode and has an affinity value of $K = 8.9 \times 10^4 \text{ M}^{-1}$. We showed with ϕX174 double-stranded DNA that the corresponding ^{99m}Tc complexes induce a significant amount of dsb, whereas non-DNA-binding $[\text{TcO}_4]^-$ and non-radioactive Re compounds did not. These results indicate that the Auger electron emitter ^{99m}Tc can induce dsb in DNA when decaying in its direct vicinity and this implies potential for systemic radiotherapy with ^{99m}Tc complexes.

Introduction

Radiopharmaceuticals containing ^{99m}Tc or other nuclides are one of the mainstays of modern diagnostic medicine. However, the use of radionuclides for therapeutic applications remains limited.^[1,2] The concept of targeted radionuclide therapy essentially relies on high-energy β^- or α emitters. The therapeutic effect is based on the high linear energy transfer (LET) of these particles which leads to the formation of cytotoxic reactive oxygen species (ROS) or direct damage to vital cellular biomolecules, ultimately inducing necrotic or apoptotic cell death. One of the major limitations of this kind of therapy is the low accumulation of the radiopharmaceutical in the targeted cells. In addition, due to the relatively high penetration range of β^- and α particles in tissue (up to 12 mm and 100 μm , respectively), healthy neighboring cells are also damaged. Accompanying γ emission (if present) deposits a high dose in the bone marrow and therefore limits the total amount of applicable activity. Finally, radioactive drug metabolites induce unwanted damage to the kidneys and/or liver during excretion. Frequently, bone marrow or kidney toxicity becomes dose-limiting before sufficiently high doses for antitumor activity can be reached.^[3,4]


Recently, the use of high LET, low energy electron emitting nuclides for radiotherapeutic applications has received much attention. It has been shown that, due to their short penetration range in tissue (from a few \AA up to 10 μm depending on their energy), low-energy Auger electrons, as well as the residually charged nuclei, produce highly dense irradiation in the immediate vicinity of the decay site.^[5–7] Cell experiments

showed that Auger emitters located outside the cell nucleus were relatively nontoxic, while intranuclear decay at the DNA caused pronounced high-LET-type damage to the nucleus, either through direct energy deposition or indirectly through the formation of highly reactive ROS, that led ultimately to cell death.^[8–10] The therapeutic potential of Auger electron emitting radionuclides has already been demonstrated by several groups. In particular, the induction of DNA damage such as DNA-double-strand breaks (dsb), which are a good indicator of cytotoxicity and the in vitro cytotoxic effects of ^{111}In , ^{125}I , ^{123}I , and ^{195m}Pt , have been reported.^[11–13] Behr and co-workers have further shown in different in vivo experiments that, at equitoxic doses, the therapeutic efficacy of internalizing monoclonal antibodies (mAbs) labeled with Auger electron emitters, such

[a] Dr. P. Häfliger, N. Agorastos, Dr. B. Spingler, Prof. Dr. R. Alberto
Institute of Inorganic Chemistry, University of Zürich
Winterthurerstraße 190, 8057 Zürich (Switzerland)
Fax: (+41) 1-635-6803
E-mail: ariel@aci.unizh.ch

[b] Dr. O. Georgiev
Institute of Molecular Biology, University of Zürich
Winterthurerstraße 190, 8057 Zürich (Switzerland)

[c] Dr. G. Viola
Department of Pharmaceutical Sciences, University of Padova
via Marzolo 5, 35131 Padova (Italy)

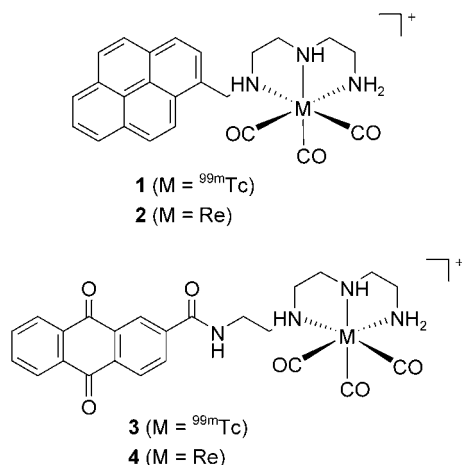
 Supporting Information for this article is available on the WWW under <http://www.chembiochem.org> or from the author: Tables of X-ray crystallographic data collection and structure refinement for complexes 2 and 4.

as ^{125}I or ^{111}In , is superior to that of internalizing mAbs labeled with conventional β^- emitters.^[14,15]

Besides its well-known γ radiation, which is used in diagnosis, $^{99\text{m}}\text{Tc}$ also emits an average of 1.1 conversion electrons and 4 Auger or Coster–Kronig electrons per decay.^[16] The $^{99\text{m}}\text{Tc}$ Auger electrons with the highest theoretical probability of inducing DNA dsb, according to Ftacnikova and Bohm, are listed in Table 1.^[7] The theoretical radiotoxicity of $^{99\text{m}}\text{Tc}$ has been calculated through its ability to induce dsb in DNA when located in its direct vicinity but has never been verified experimentally.^[6,7] We present in this paper experimental evidence that $^{99\text{m}}\text{Tc}$ complexes with pendant DNA-binding moieties induce in vitro DNA-double-strand breaks. For this purpose, the bifunctional compounds **1** and **3** (Scheme 1) were synthesized. They comprise a pendant DNA binder and a $^{99\text{m}}\text{Tc}$ -tricarbonyl core coordinated to a triamine ligand. The interaction of the Re analogues of both compounds with double-stranded DNA was studied by UV/Vis spectroscopy and linear dichroism. Finally, we analyzed the ability of the $^{99\text{m}}\text{Tc}$ complexes to induce in vitro DNA-double-strand breaks by using ϕX174 double-stranded (ds) DNA.

Table 1. Average energy, yield/decay, and penetration range in tissue of the main electrons emitted by $^{99\text{m}}\text{Tc}$. (CK = Coster–Kronig; MMX, MXy, and NNx = type of electron as defined in the literature).^[16]

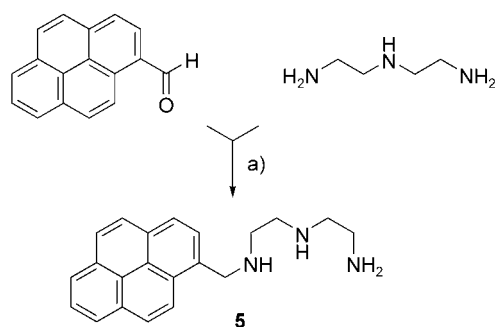
Electron type	Average energy [eV]	Yield/decay	Range in tissue [nm]
CK MMX	116	0.75	6
Auger MXy	226	1.1	10.5
CK NNx	33	1.98	2



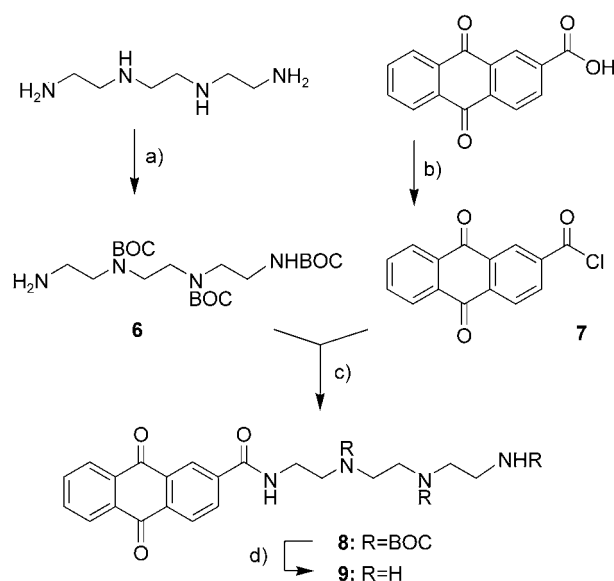
Scheme 1. Basic structures of the bifunctional $^{99\text{m}}\text{Tc}$ -tricarbonyl complexes.

Results and Discussion

The ligands **5** and **9** have been synthesized according to Schemes 2 and 3 in good yields by using standard protecting-group procedures. They are bifunctional and comprise a diethylene triamine unit for tridentate coordination to the fac-



Scheme 2. Synthesis of compound **5**. a) 1. 1-pyrenecarboxaldehyde, EtOH/ CH_2Cl_2 , 2. NaBH_4 , EtOH, overall yield = 44%.



Scheme 3. Synthesis of compound **9**. a) 1. Dde, EtOH, 2. $(\text{BOC})_2\text{O}$, EtOH, 3. hydrazine, EtOH, overall yield = 77%; b) SOCl_2 , DMF, yield = 67%; c) Et_3N , CH_2Cl_2 , yield = 91%; d) TFA, CH_2Cl_2 , yield > 98%. BOC = tert-butoxycarbonyl, Dde = 2-acetyl-5,5-dimethyl-cyclohexane-1,3-dione, DMF = N,N-dimethylformamide, TFA = trifluoroacetic acid.

$[\text{M}(\text{CO})_3]^+$ moiety (M = Re, $^{99\text{m}}\text{Tc}$) and an aromatic ring system for interaction with DNA. The coordinating triamine ligand has been chosen since it forms a small complex with a monocationic charge that should support electrostatic interaction to the negatively charged backbone of DNA. Both ligands react in water or MeOH with $[\text{ReBr}_3(\text{CO})_3]^{2-}$ (in water $[\text{Re}(\text{OH})_2_3(\text{CO})_3]^+$) to form the complexes $[\text{Re}(\mathbf{5})(\text{CO})_3]^+$ (**2**) and $[\text{Re}(\mathbf{9})(\text{CO})_3]^+$ (**4**) in quantitative yields. The d^6 nature of the M^I center renders the complexes very robust and no decomposition was observed even at low pH values or under physiological conditions.

Complexes **2** and **4** have three chiral centers, two of which are independent. Thus, the complexes can exist as two diastereomeric pairs of enantiomers, which can be clearly identified by HPLC in the case of compound **2** (Figure 1). On the other hand, only one diastereomeric pair seems to be preferentially formed in the case of complex **4** (Figure 2). Crystal structures of one isomer of compounds **2** and **4** could be obtained.

ORTEP representations are given in Figures 3 and 4, respectively.^[17] Further details are given in the Supporting Information. HPLC analysis showed that the crystal of complex **2** corre-

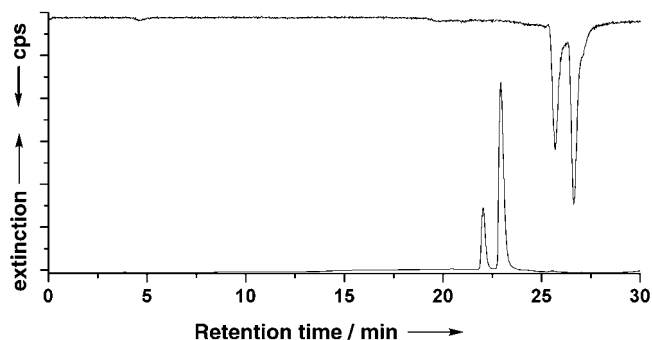


Figure 1. HPLC traces of complexes **1** and **2** with UV detection (bottom) and radiodetection (top), respectively. The difference in retention time is due to the detector separation.

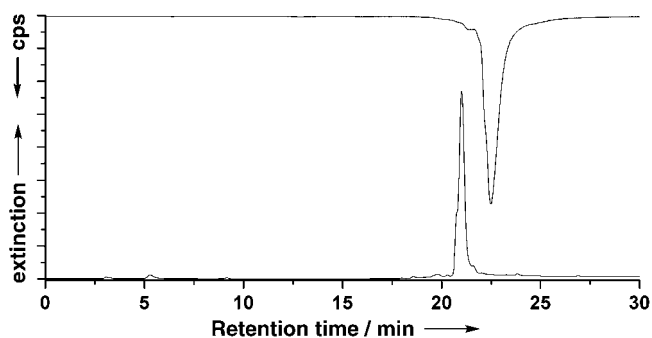


Figure 2. HPLC traces of complexes **3** and **4** with UV detection (bottom) and radiodetection (top), respectively. The difference in retention time is due to the detector separation.

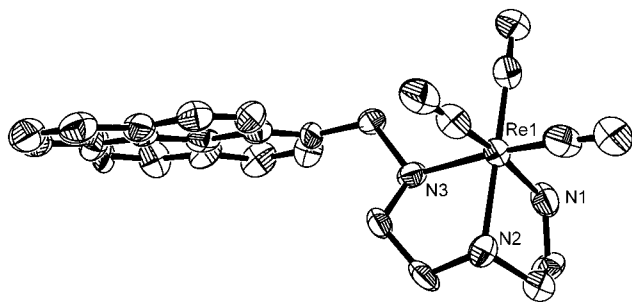


Figure 3. ORTEP plot of the monocationic complex **2**. Ellipsoids are shown with 50% probability.

sponds to the second peak in the HPLC trace. The structures clearly show for both complexes that the two functions, the DNA-binding portion and the tricarbonyl rhenium unit, point away from each other, so the latter should not sterically affect the DNA binding of the aromatic systems.

Complexes **1** and **3** have been synthesized in quantitative yield by treating ligands **5** and **9** in water with $[\text{}^{99\text{m}}\text{Tc}(\text{OH})_2]_3^-$

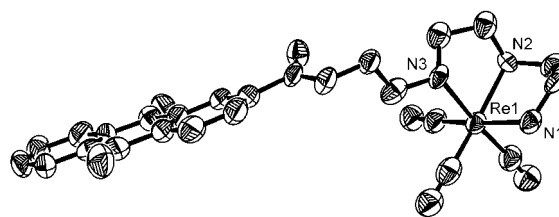


Figure 4. ORTEP plot of the monocationic complex **4**. Ellipsoids are shown with 50% probability.

$(\text{CO})_3]^+$ prepared directly from $[\text{}^{99\text{m}}\text{TcO}_4]^-$ as previously described.^[18] Comparison of the HPLC traces of the $^{99\text{m}}\text{Tc}$ complexes (radiodetection) and the Re analogues (UV detection) confirmed the identity of the two compounds. The traces are shown in Figures 1 and 2. Both complexes displayed a high stability over time and with respect to temperature changes.

Interaction with ds DNA

The analysis of the DNA binding of **2** and **4** was performed by titration with calf-thymus DNA and monitoring with UV/Vis spectroscopy. Series of spectra of complexes **2** and **4** with an increasing amount of DNA are shown in Figures 5 and 6. Complex **2** displays a strong hypochromism and a large red shift (12 nm) of the absorption maximum upon interaction with DNA. Moreover, an isosbestic point at 349 nm is clearly visible for DNA/complex ratios smaller than 4.5:1. Above this value, it shifts to 342 and 345 nm. These phenomena indicate that one type of **2**-DNA complex is formed almost exclusively under these conditions.

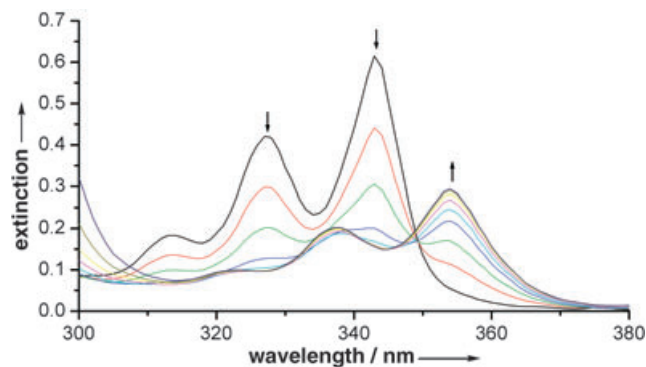


Figure 5. Binding isotherms of a solution containing 1.26×10^{-5} M complex **2**, 10 mM tris(hydroxymethyl)aminomethane (Tris) buffer (pH 7.4), 50 mM NaCl, and 0, 1, 2, 3.5, 5, 7, 10, 17, and 35 equivalents of calf-thymus DNA. (For clarity, not all recorded spectra are displayed.)

In the case of complex **4**, addition of DNA also induced hypochromism but only a weak red shift of the absorption maximum in the UV/Vis spectrum (4 nm). The isosbestic point at 363 nm for DNA/complex ratios smaller than 6:1 shifts to 355 nm for higher ratios. The formation of an isosbestic point again indicates the formation of only one type of **4**-DNA complex. However, in contrast with **2**, the magnitude of the batho-

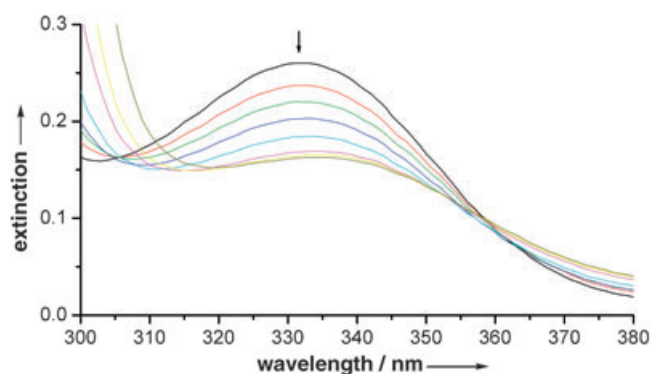


Figure 6. Binding isotherms of a solution containing 4.95×10^{-5} M compound **4**, 10 mM Tris buffer (pH 7.4), 50 mM NaCl, and 0, 1, 2, 3, 5, 10, 15, and 30 equivalents of calf-thymus DNA. (For clarity, not all recorded spectra are displayed.)

chromic shift suggests external (that is, not intercalative) binding to the DNA, since shifts are usually more pronounced for compounds that bind by intercalation than for those binding to a groove.^[19–21]

A strong interaction of complexes **1** and **3** with DNA is crucial in order to efficiently induce as many double-strand breaks as possible at submicromolar concentrations. In order to determine the affinity constant for the DNA interaction of these complexes with DNA, the UV/Vis spectra were redrawn in the form of Scatchard plots (r/C_{free} versus r) and subsequently fitted with the model of McGhee and von Hippel, which is widely used for the analysis of the interaction of drugs with DNA.^[22] The corresponding plots and fits are shown in Figure 7. Calculated DNA affinity constants, K , and neighbor-exclusion parameters, n , for compounds **2** and **4**, as well as for their free ligands **5** and **9** (spectra shown in the Supporting Information) are summarized in Table 2.

Table 2. Calculated DNA affinity constants (K), neighbor-exclusion parameters (n), and goodness of fit values (R^2) for compounds **2**, **4**, **5**, and **9**.

Compound	K [M^{-1}]	n	R^2
2	$1.1(\pm 0.1) \times 10^6$	4.4 ± 0.2	0.95
4	$8.9(\pm 0.9) \times 10^4$	3.9 ± 0.3	0.86
5	$2.7(\pm 0.3) \times 10^6$	4.0 ± 0.3	0.97
9	$1.0(\pm 0.1) \times 10^5$	4.0 ± 0.2	0.92

The equilibrium constants between underivatized pyrene or the anthraquinone derivative *N*-(4-aminobutyl)-2-anthraquinonecarboxamide and DNA are reported to be approximately $1 \times 10^5 \text{ M}^{-1}$ and $7.7 \times 10^4 \text{ M}^{-1}$, respectively.^[23,24] Compound **5** carries, in addition to the pyrene moiety, two or three positively charged amines which can electrostatically increase the interaction to the negatively charged DNA phosphate backbone. Correspondingly, the affinity of **5** is 30 times higher than for pyrene alone. Not surprisingly, this affinity is reduced when compound **5** is coordinated to the $[\text{Re}(\text{CO})_3]^+$ moiety. After coordination, **2** is only monocationic and some steric interactions might reduce the stability further. However, the affinity value is still

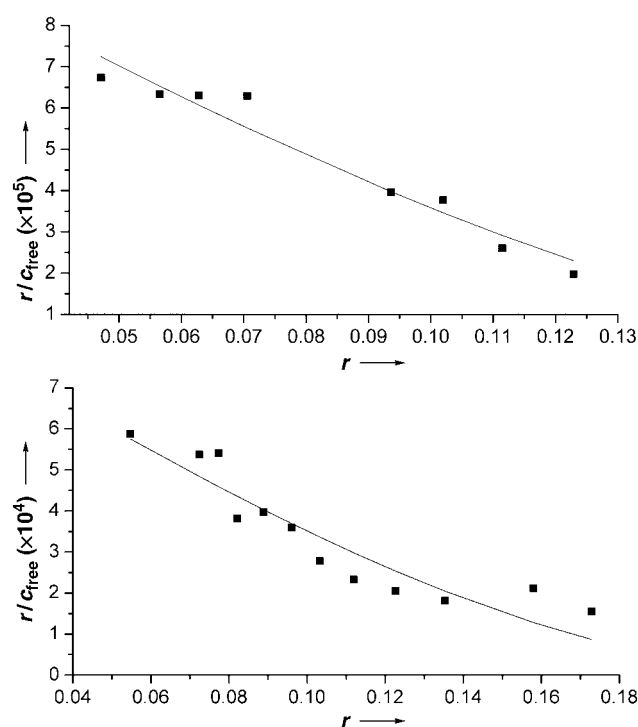


Figure 7. 342 nm and 333 nm Scatchard plots (dots) of the binding of **2** (top) and **4** (bottom) with calf-thymus DNA fitted with the model of McGhee and von Hippel (line). $r = C_{(\text{ical-bound})}/C_{(\text{DNA})}$ with $C_{(\text{DNA})} = 25.2$ (**7a**) and $49.5 \mu\text{M}$ (**7b**).

$$C_{\text{free}} = C_{(\text{ical-bound})} - C_{(\text{ical-bound})}$$

10 times larger than for pyrene alone. The situation is slightly different with **9** or **4**, but the same relative tendency can be observed. The stability constant of the free bifunctional ligand **9**, which is a di- or trication, was found to be $1.0 \times 10^5 \text{ M}^{-1}$, about 1.3 times higher than the monocationic compound *N*-(4-aminobutyl)-2-anthraquinonecarboxamide. Correspondingly, the DNA affinity of the monocationic metal complex **4** is slightly lower ($8.9 \times 10^4 \text{ M}^{-1}$).

However, the stability constants observed for complexes **2** and **4** are sufficiently high to allow strong binding of both complexes to DNA. It is easily estimated that more than 99% of the molecules are bound to DNA, even at the submicromolar concentrations required when working with ^{99m}Tc.

Linear dichroism

Large aromatic systems interact with DNA through two general modes: 1) in a groove-binding fashion and 2) through intercalation. Several methods are known to probe the interaction of these types of molecules with DNA.^[25] It has been pointed out that one single method is not sufficient to accurately prove which binding mode is favored.^[26] For this reason, we measured the linear dichroism (LD) at different complex/DNA ratios for complexes **2** and **4**, in addition to the UV/Vis spectra. The LD signal of **2** is negative at all mixing ratios in the wavelength region where only the polyaromatic unit absorbs (310–370 nm; Figure 8). This indicates an induced orientation of the chromophore upon binding to DNA. A small increase of the LD signal

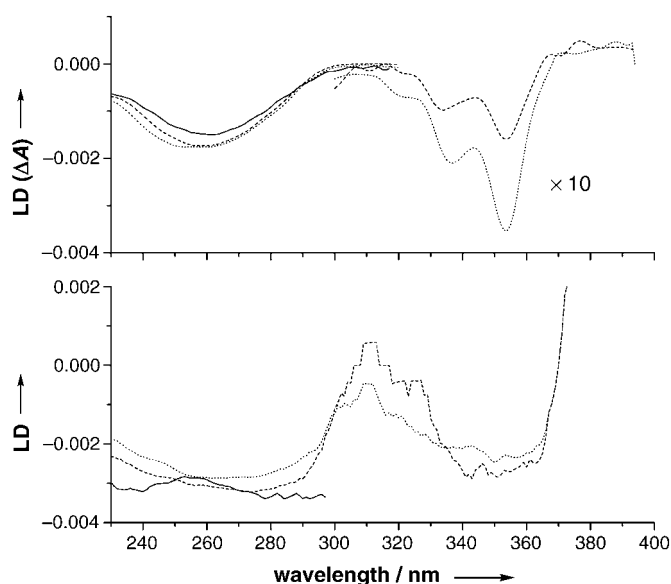


Figure 8. Linear dichroism (LD) and reduced linear dichroism (LD_r) spectra of DNA (230–310 nm) and complex **2** (310–370 nm) at complex/DNA ratios of 0.04 (----) and 0.08 (.....) or of DNA only (—).

intensities in the absorption band of the DNA bases (260 nm) was also observed and suggests that the ability of the DNA molecules to orient along the flow lines is increased upon binding to this compound.

The reduced LD spectrum (LD_r) provides further information on the average orientation of the transition moment of the pyrene moiety relative to those of the DNA bases and allows us to distinguish between homogeneous and heterogeneous binding. A nearly constant value of LD_r over the range 340–360 nm was observed (Figure 8), which unambiguously implies an almost exclusive intercalation of **2** into DNA.^[27,28]

It is expected that compound **4** interacts with DNA in an intercalative way, as is known for purely organic anthraquinone derivatives.^[29,30] However, even at a complex/DNA ratio of 0.2, no induced linear dichroism signal in the region where compound **4** absorbs (315–360 nm) is visible, despite a significant absorption in this region (Figure 9). This observation indicates that this compound does not intercalate DNA and is probably bound to a groove of the DNA. Alternatively, the orientation angle between the complex and the DNA axis could be about 55°, which is the angle at which the LD_r value is 0.^[27,28] Moreover, a remarkable reduction of the LD band in the DNA absorption region (260 nm) with increasing concentrations of **4** is indicative of a reduced orientation of the DNA along the flow lines.

DNA double strand break experiments

A convenient method to analyze the formation of DNA dsb is based on the use of circular ds DNA. The induction of a double-strand break to either a supercoiled circular or an open circular form of DNA results in the formation of a linear molecule, which can easily be detected by gel electrophoresis.

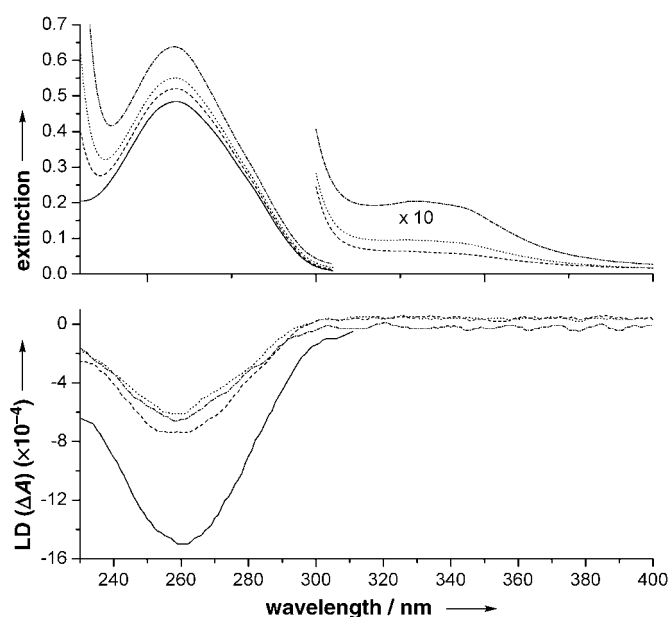


Figure 9. Absorption and linear dichroism (LD) spectra of DNA (230–310 nm) and complex **4** (315–360 nm) at complex/DNA ratios of 0.04 (----) 0.08 (.....), and 0.2 (-.-.-) or of DNA only (—).

The ability of compounds **1** and **3** to induce DNA dsb was determined by their incubation with a mixture of supercoiled and open circular ϕ X174 DNA in a buffered aqueous solution. The “mechanical” formation of open circular DNA through single-strand breaks (ssb) can hardly be omitted since the solutions are stirred at room temperature for three days under nonsterile conditions. In order to avoid saturation of the DNA molecules with unlabeled bifunctional ligands **5** and **9**, compounds **1** and **3** were purified by HPLC prior to use. Non-DNA-binding $[^{99m}\text{TcO}_4]^-$ and the nonradioactive Re complexes **2** and **4** were used as reference compounds. Subsequent gel electrophoresis and staining with ethidium bromide allowed detection and quantification of dsb by the measurement of the fluorescence intensities of the different bands. The traces obtained are displayed in Figure 10. The choice of an appropriate amount of radioactivity turned out to be a crucial factor in these experiments. Whereas substantially lower amounts of ^{99m}Tc did not reveal dsb but showed a picture similar to the one displayed in trace 1, higher amounts of ^{99m}Tc resulted in multiple dsb that led to partial DNA fragmentation and “smearing” of the traces. This is positive with the perspective of applying the concept in therapy but does not give a clear picture of the molecular events responsible for the “disappearing” of the DNA from the gel.

Figure 10 shows that compounds **1** and **3** did induce dsb in 15 and 20%, respectively, of the ϕ X174 molecules, while non-DNA-binding $[^{99m}\text{TcO}_4]^-$ and nonradioactive **2** did not. This implies that dsb are induced by Auger and Coster-Kronig electrons emitted by ^{99m}Tc only when the nuclide is located in the near vicinity of the DNA. The induction of dsb by accompanying γ emission can be ruled out since photons, due to their low LET, only negligibly interact with DNA over such a short distance. The amount of supercoiled DNA in traces 3 and 4 de-

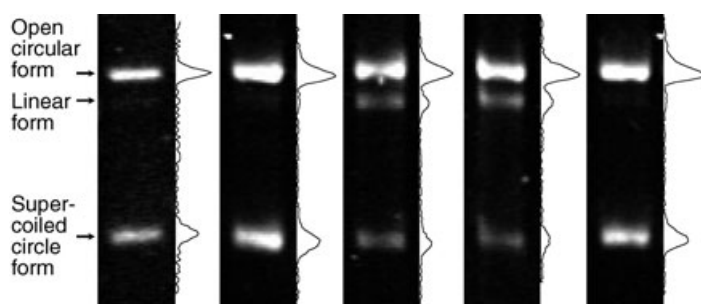


Figure 10. Electrophoresis of ϕ X174 DNA (100 ng) after 24 h incubation in Tris buffer (50 mM, pH 7.4, 50 μ M) with (from left to right): buffer only, non-DNA-binding $^{99m}\text{TcO}_4^-$ (15 MBq; $\approx 1.5 \times 10^{-8}$ M), DNA-binding pyrene ^{99m}Tc complex **1** (15 MBq; $\approx 0.2 \times 10^{-8}$ M), DNA-binding anthraquinone ^{99m}Tc complex **3** (2.3 MBq; $\approx 0.2 \times 10^{-8}$ M), and nonradioactive DNA-binding Re complex **2** (2×10^{-8} M; trace similar to the one obtained after incubation with the nonradioactive compound **4**). The fluorescence intensity of the bands is displayed on the right hand side of each trace.

creased but is still present. In principle, the appearance of the linear form can result from one dsb induced in the open circular or in the supercoiled form. The form in which it finally occurs is biologically not relevant. Linearization could also be induced by multiple ssb occurring within about 30–40 base pairs on opposite strands. The ϕ X174 DNA comprises about 5000 base pairs. However, when it is considered that not every DNA molecule has been damaged (the supercoiled form is still left), this pathway of linearization appears unlikely. Furthermore, induction of one or more additional dsb in an already linearized molecule would fragment the DNA and increase the background noise. We found, under our conditions, a maximum of 20% dsb. If it is assumed that a second double-strand break in these linearized DNA molecules gave about 4% loss of DNA on the gel, this is an amount that is difficult to quantify with our experimental method.

Interestingly, the double-strand-break yield per decay is about 10 times higher for compound **3** (0.05) than for compound **1** (0.005). The anthraquinone moiety present in the former compound might be able to improve DNA damage through a redox process initiated by the capture of an Auger electron, in a way similar to that proposed by Armitage and co-workers for the induction of DNA damage upon photoactivation of anthraquinone derivatives.^[24] The double-strand-break yields per decay obtained are much lower than the theoretical values calculated by Ftacnikova and Bohm (0.86)^[7] or Humm and Charlton (0.43)^[6] for a ^{99m}Tc atom incorporated in a DNA base (like I in IdU). In our experiments, the ^{99m}Tc atom was, however, located a few ångströms off the DNA surface. This might account for the lower yields obtained in our experiments.

In order to determine whether dsb are induced preferentially through a direct or an indirect mechanism, the experiments were also performed in the presence of the radical scavengers mannitol and thiourea. These should neutralize ROS and reduce the amount of indirectly induced damage. However, the presence of these compounds did not significantly modify the obtained results. Thus, the dsb seem to be mainly induced through the direct action of emitted electrons or through dif-

fusion-controlled reaction of ROS with DNA. Only these mechanisms are possible in the presence of radical scavengers.

Conclusion

In conclusion, we have demonstrated experimentally that Auger electron emitting ^{99m}Tc induces double-strand breaks in DNA when decaying in its direct vicinity, a result implying that ^{99m}Tc might possess potential for systemic radiotherapy in addition to its widely known role in diagnosis. The ^{99m}Tc labeling of compounds that selectively target the cellular DNA of specific cells is the molecular basis for such a strategy. The future challenge is the evaluation of carrier compounds for ^{99m}Tc that efficiently target cellular DNA.

Experimental Section

Materials and methods: Chemicals and solvents were purchased from commercial suppliers and used without further purification. All reactions were performed under N_2 or Ar. $\text{Na}^{99m}\text{TcO}_4$ was eluted from a $^{99}\text{Mo}/^{99m}\text{Tc}$ generator (Mallinckrodt) in 0.9% saline. Calf-thymus DNA was purchased from Fluka and purified by multiple phenol extraction steps. ϕ X174 ds DNA was purchased from Promega and used without further purification.

^1H and ^{13}C NMR spectra were recorded on Varian Gemini 300 (300 and 75 MHz, respectively) or Bruker DRX500 (500 and 125 MHz, respectively) spectrometers. The reported chemical shifts (δ in ppm) are relative to the solvent protons used for reference. TLC was performed on Merck silica gel 60 R_{254} plates. The compounds were visualized with UV light (254 nm) or Schittler reagent.^[31] HPLC was performed on a Merck L7000 system with a Macherey–Nagel EC 250/3 Nucleosil 100–5 C18HD column for nonradioactive compounds and a Macherey–Nagel EC 250/3 Nucleosil 100–5 C18 column for radioactive compounds. HPLC solvents were 0.1% trifluoroacetic acid (solvent A) and HPLC-grade MeOH (solvent B). Gradient: 0–3 min: 100% A; 3.1–9 min: 75% A, 25% B; 9.1–20 min: linear gradient from 66% A, 34% B to 100% B; 20–28 min: 100% B; 28.1–30 min: 100% A. Flow rate: 0.5 mL min^{-1} . Detection wavelength: 250 nm. Preparative HPLC: Varian Pro Star system with a Macherey–Nagel VP 250/40 Nucleosil 100–7 C18 column and a flow rate of 40 mL min^{-1} . UV/Vis spectra were recorded on a Perkin–Elmer Cary 50 spectrometer equipped with a Peltier thermostat. Linear dichroism (LD) spectra were recorded in a “flow cell” on a Jasco J500A spectropolarimeter equipped with an IBM PC and a Jasco J interface. The determination and interpretation of the data were performed as described in previous publications.^[32,33]

X-ray data collection was performed on a STOE IPDS diffractometer. Suitable crystals were covered with Paratone N oil and mounted on top of a glass fiber. Data were collected at 183(2) K by using graphite-monochromated $\text{Mo}_{\text{K}\alpha}$ radiation ($\lambda = 0.71073$ Å). 8000 reflections distributed over the whole limiting sphere were selected by the program SELECT and used for unit-cell parameter refinement with the program CELL. Data were corrected for Lorentz and polarization effects as well as for absorption (numerical). Structures were solved with direct methods by using the SHELXS-97 or SIR97 programs and were refined by the full-matrix least-squares methods on F^2 with the SHELXL-97 program.

N-(2-Aminoethyl)-N'-pyrene-1-ylmethylethane-1,2-diamine (5): Pyrene-1-carbaldehyde (1.08 g, 4.69 mmol) and (1.452 g, 1.528 mL, 14.07 mmol) diethylenetriamine were dissolved in EtOH (50 mL). CH₂Cl₂ was added until the solution became clear. After molecular sieves (5 g, 3 Å pore diameter) had been added, the solution was stirred for 36 h at RT. The solution was then cooled to 0 °C, and NaBH₄ (355 mg, 9.38 mmol) was added in small portions. After 12 h, excess NaBH₄ was quenched with a few drops of H₂O. The solution was filtered and dried in vacuo. The resulting oil was purified by flash chromatography (CH₂Cl₂/MeOH/25% NH₄OH, 100:30:3) to afford a light yellow oil (649 mg, 44%): ¹H NMR (CDCl₃): δ = 8.22 (d, 1H), 8.07 (d, 2H), 8.01 (m, 2H), 7.90 (m, 4H), 4.34 (s, 2H), 2.99 (s, 4H), 2.74 (t, 2H), 2.66 (t, 2H), 2.60 (t, 2H), 2.51 (t, 2H) ppm; ¹³C NMR (CDCl₃): δ = 133.4, 131.1, 130.6, 130.5, 128.9, 127.5, 127.3, 126.9, 125.8, 125.0, 124.9, 124.8, 124.6, 124.5, 123.0, 51.1, 50.6, 48.5, 40.6 ppm; MS (ESI): *m/z*: 318.27 [M+H]⁺ (*m/z* calcd for [C₂₁H₂₄N₃]⁺: 318.20); HPLC: *R*_t = 17.8 min; TLC: *R*_f = 0.15 (CH₂Cl₂/MeOH/25% NH₄OH, 100:30:3).

(2-Aminoethyl)-(2-(tert-butoxycarbonyl)-(2-tert-butoxycarbonylaminoethyl)amino)ethyl)carbamic acid tert-butyl ester (6): 2-Acetyl-5,5-dimethyl-cyclohexane-1,3-dione (Dde) (0.788 g, 4.32 mmol) in EtOH (10 mL) was slowly added to an ice-cooled solution of *N,N'*-bis-(2-aminoethyl)-ethane-1,2-diamine (1.265 g, 1.3 mL, 8.65 mmol) dissolved in EtOH (10 mL). The reaction mixture was stirred overnight at RT. After completion of the reaction, the solvent was removed in vacuo. The resulting crude product (2.6 g) was dissolved in EtOH (20 mL) and cooled to 0 °C. Di-*tert*-butyl-pyrocyanate ((BOC)₂O, 7 g) in EtOH (20 mL) was then slowly added to the reaction mixture, which was subsequently stirred overnight at RT. Excess of di-*tert*-butyl-pyrocyanate ((BOC)₂O) was quenched with H₂O (1 mL) and subsequent stirring at 50 °C for 30 min. A 25% aqueous hydrazine solution (10 mL) was then added to the reaction mixture and stirring was continued for 4 h at RT. The solvent was removed in vacuo. The resulting oil was purified by flash chromatography (EtOAc/MeOH/25% NH₄OH, 100:10:1) to yield a colorless oil (1.47 g, 77% based on the quantity of Dde): ¹H NMR (CDCl₃): δ = 4.13–4.11 (brs, 1H), 3.32 (br, 10H), 2.86 (br, 2H), 2.23 (br, 2H), 1.46 (s, 18H), 1.43 (s, 9H) ppm; ¹³C NMR (CDCl₃): δ = 158.3, 157.2, 81.3, 79.9, 49.8–46.6, 40.1, 28.8 ppm; MS (ESI): *m/z*: 447.12 [M+H]⁺ (*m/z* calcd for [C₂₁H₄₃N₄O₆]⁺: 447.31); TLC: *R*_f = 0.12 (EtOAc/MeOH/25% NH₄OH, 100:10:1).

9,10-Dioxo-9,10-dihydroanthracene-2-carbonyl chloride (7): A solution containing 9,10-dioxo-9,10-dihydroanthracene-2-carboxylic acid (500 mg) and a few drops of DMF in SOCl₂ (7.5 mL) was heated under reflux for 4 h. Excess SOCl₂ was removed under high vacuum. Recrystallization from CH₂Cl₂/EtOAc (9:2) afforded **7** (360 mg, 67%) as light-yellow needles: ¹H NMR ([D₆]DMSO): δ = 8.66 (s, 1H), 8.43 (m, 1H), 8.31 (m, 1H), 8.23 (d, 2H), 7.97 (t, 2H) ppm; ¹³C NMR (CDCl₃): δ = 182.3, 182.2, 164.9, 135.9, 135.4, 134.6, 134.4, 134.3, 133.4, 130.3, 129.6, 128.4, 128.2, 127.3, 126.8 ppm; IR (KBr): $\tilde{\nu}(\text{CO}-\text{Cl}) = 1745 \text{ cm}^{-1}$, $\tilde{\nu}(\text{CO}) = 1674 \text{ cm}^{-1}$; elemental analysis: calcd (%) for C₁₅H₇O₃Cl: C 66.56, H 2.61; found: C 66.54, H 2.56.

(2-(tert-Butoxycarbonyl)-(2-tert-butoxycarbonylamino-ethyl)-amino-ethyl)-(2-((9,10-dioxo-9,10-dihydroanthracene-2-carbonyl)amino)ethyl)carbamic acid tert-butyl ester (8): A solution of **7** (150 mg, 0.55 mmol) in CH₂Cl₂ (5 mL) was slowly added to an ice-cooled solution of **6** (236 mg, 0.53 mmol) and Et₃N (220 μL, 1.59 mmol) in CH₂Cl₂ (7 mL). This light-yellow mixture was stirred at RT for 2 h. After removal of the solvent in vacuo, the crude product was purified by flash chromatography (CH₂Cl₂/MeOH, 100:3) to yield **8** (327 mg, 91%) as a yellow oil: ¹H NMR (CDCl₃):

δ = 8.66 (s, 1H), 8.30–8.18 (m, 4H), 7.76–7.71 (m, 2H), 4.90 (brs, 1H), 3.54 (brs, 2H), 3.48 (brs, 2H), 3.32 (brs, 10H), 1.38 (s, 9H), 1.36 ppm (s, 18H); ¹³C NMR (CDCl₃): δ = 182.8, 182.6, 165.2, 156.2, 136.1, 135.6, 134.7, 134.6, 134.5, 133.66, 133.58, 133.51, 128.7, 127.62, 127.54, 127.48, 77.2, 49.6–44.1, 39.8–38.9 ppm; MS (ESI): *m/z*: 680.20 [M]⁺ (*m/z* calcd for [C₃₆H₄₈N₄O₉]⁺: 680.34); HPLC: *R*_t = 24.5 min; TLC: *R*_f = 0.20 (CH₂Cl₂/MeOH, 100:3).

9,10-Dioxo-9,10-dihydroanthracene-2-carboxylic acid (2-(2-(2-aminoethylamino)ethylamino)ethyl)amide (9): Trifluoroacetic acid (3 mL) was added to a solution of **8** (607 mg, 0.89 mmol) in CH₂Cl₂ (7 mL). This mixture was stirred at RT for 5 h. After the solvent had been removed in vacuo, the product was dried overnight in high vacuum to yield compound **9** (339 mg, >98% (HPLC)) as a light-yellow oil: ¹H NMR (D₂O): δ = 8.01 (s, 1H), 7.85 (d, 1H), 7.78 (m, 3H), 7.63 (m, 2H), 3.77 (t, 2H), 3.57 (brs, 4H), 3.50 (m, 2H), 3.4 (m, 4H) ppm; ¹³C NMR (CDCl₃): δ = 183.1, 182.9, 168.1, 137.3, 135.0, 134.4, 132.7, 132.4, 132.0, 126.8–127.5, 125.5, 47.8, 44.5, 43.3, 43.0, 36.4, 35.2 ppm; MS (ESI): *m/z*: 380.80 [M+H]⁺ (*m/z* calcd for [C₂₁H₂₅N₄O₃]⁺: 381.19); HPLC: *R*_t = 17.9 min.

Re complexes: General procedure: A solution containing [Re(Br)₃(CO)₃][Et₄N]₂ (0.30 mmol), prepared as previously described,^[34,35] the organic molecule (0.30 mmol), and Et₃N (1 mmol) in MeOH (10 mL) was stirred under reflux until completion of the reaction. After removal of the solvent in vacuo, the resulting crude product was purified by preparative HPLC. Yields prior to purification were higher than 98% according to analytical HPLC. Final yields after purification were smaller due to loss during the purification procedure.

Complex 2: Yield = 62%; ¹H NMR (second diastereomer; CD₃CN): δ = 8.40 (d, 1H), 8.26 (m, 5H), 8.2–8.05 (m, 3H), 5.84 (brs, 1H), 5.67 (brs, 1H), 5.25 (brs, 1H), 5.14 (q, ¹*J* = 24, ²*J* = 8 Hz, 1H), 4.90 (q, ¹*J* = 24, ²*J* = 15 Hz, 1H), 4.26 (brs, 1H), 3.23 (m, 1H), 2.94 (m, 3H), 2.79 (m, 1H), 2.63 (m, 1H), 2.4 (brs, 2H) ppm; ¹³C NMR (second diastereomer; CD₃CN): δ = 196.9, 196.5, 195.0, 132.5, 132.3, 131.7, 131.6, 130.6, 129.7, 129.3, 128.9, 128.4, 127.5, 126.7, 126.5, 126.0, 125.6, 125.4, 123.8, 59.6, 54.5, 53.7, 49.9, 40.6 ppm; MS (ESI): *m/z*: 587.81 [M]⁺ (*m/z* calcd for C₂₄H₂₃N₃O₃Re: 588.13); HPLC: *R*_t = 22.2 and 23.2 min.

Complex 4: Yield: 78%; ¹H NMR (second diastereomer; D₂O): δ = 8.01 (s, 1H), 7.85 (d, 1H), 7.78 (m, 3H), 7.63 (m, 2H), 3.77 (t, 2H), 3.57 (brs, 4H), 3.5 (m, 2H), 3.4 (m, 4H) ppm; ¹³C NMR (second diastereomer; D₂O, 125 MHz): δ = 183.1, 182.9, 168.1, 137.3, 135.0, 134.4, 132.7, 132.4, 132.0, 126.8–127.5, 125.5, 47.8, 44.5, 43.3, 43.0, 36.4, 35.2 ppm; MS (ESI): *m/z*: 651.53 [M]⁺ (*m/z* calcd for C₂₄H₂₄N₄O₆Re: 651.12); HPLC: *R*_t = 21.7 min.

^{99m}Tc complexes: General procedure: A 10-mL vial containing a 10⁻⁴ or 10⁻⁵ M aqueous solution (100 μL) of the appropriate ligand was sealed and flushed with N₂. After addition of a saline solution (900 μL) containing about 10⁻⁷ M *fac*-[^{99m}Tc(OH)₂]₃(CO)₃⁺, prepared as previously described,^[18] the vial was heated to 90 °C for 30 min. The reaction solution was then cooled in an ice bath and the mixture was analyzed by HPLC with γ detection. **Complex 1:** HPLC: *R*_t = 25.8 and 26.7 min. **Complex 3:** HPLC: *R*_t = 24.6 min.

Acknowledgements

We thank Mallinckrodt Med. BV, Petten, The Netherlands, for financial support.

Keywords: Auger electrons · DNA damage · intercalation · radiotherapy · technetium

- [1] K. Schwochau, *Technetium—Chemistry and Radiopharmaceutical Applications*, Wiley-VCH, Weinheim, 2000.
- [2] C. B. Sampson, *Textbook of Radiopharmacy*, 3rd ed., Gordon and Breach, Amsterdam, 1999.
- [3] T. M. Behr, R. M. Sharkey, M. E. Juweid, R. M. Dunn, R. C. Vagg, Z. L. Ying, C. H. Zhang, L. C. Swayne, Y. Vardi, J. A. Siegel, D. M. Goldenberg, *J. Nucl. Med.* **1997**, *38*, 858–870.
- [4] R. D. Blumenthal, R. M. Sharkey, D. M. Goldenberg in *Cancer Therapy with Radiolabeled Antibodies* (Ed.: D. M. Goldenberg), CRC Press, Boca Raton, 1995, pp. 295–314.
- [5] K. S. R. Sastry, *Med. Phys.* **1992**, *19*, 1361–1370.
- [6] J. L. Humm, D. E. Charlton, *Int. J. Radiat. Oncol. Biol. Phys.* **1989**, *17*, 351–360.
- [7] S. Ftacnikova, R. Bohm, *Radiat. Prot. Dosim.* **2000**, *92*, 269–278.
- [8] K. G. Hofer, *Radiat. Prot. Dosim.* **1998**, *79*, 405–410.
- [9] K. G. Hofer, *Acta Oncol.* **2000**, *39*, 651–657.
- [10] J. A. O'Donoghue, T. E. Wheldon, *Phys. Med. Biol.* **1996**, *41*, 1973–1992.
- [11] M. A. Walicka, S. J. Adelstein, A. I. Kassis, *Radiat. Res.* **1998**, *149*, 142–146.
- [12] M. W. Beckmann, A. Scharl, B. J. Rosinsky, J. A. Holt, *J. Cancer Res. Clin. Oncol.* **1993**, *119*, 207–214.
- [13] J. Dahm-Daphi, C. Sass, W. Alberti, *Int. J. Radiat. Biol.* **2000**, *76*, 67–75.
- [14] T. M. Behr, M. Behe, M. Lohr, G. Sgouros, C. Angerstein, E. Wehrmann, K. Nebendahl, W. Becker, *Eur. J. Nucl. Med.* **2000**, *27*, 753–765.
- [15] T. M. Behr, G. Sgouros, V. Vougioukas, S. Memtsoudis, S. Gratz, H. Schmidberger, R. D. Blumenthal, D. M. Goldenberg, W. Becker, *Int. J. Cancer* **1998**, *76*, 738–748.
- [16] R. W. Howell, *Med. Phys.* **1992**, *19*, 1371–1383.
- [17] CCDC-231995 (2) and 250837 (4) contain the supplementary crystallographic data for this paper. These data can be obtained free of charge from The Cambridge Crystallographic Data Centre via www.ccdc.cam.ac.uk/data_request/cif.
- [18] R. Alberto, K. Ortner, N. Wheatley, R. Schibli, A. P. Schubiger, *J. Am. Chem. Soc.* **2001**, *123*, 3135–3136.
- [19] G. Behravan, M. Leijon, U. Sehlstedt, B. Norden, H. Vallberg, J. Bergman, A. Graslund, *Biopolymers* **1994**, *34*, 599–609.
- [20] W. D. Wilson, F. A. Tanius, H. J. Barton, R. L. Jones, K. Fox, R. L. Wydra, L. Strekowski, *Biochemistry* **1990**, *29*, 8452–8461.
- [21] W. D. Wilson, F. A. Tanius, R. A. Watson, H. J. Barton, A. Strekowska, D. B. Harden, L. Strekowski, *Biochemistry* **1989**, *28*, 1984–1992.
- [22] J. D. McGhee, P. H. von Hippel, *J. Mol. Biol.* **1974**, *86*, 469–489.
- [23] F. M. Chen, *Anal. Biochem.* **1983**, *130*, 346–352.
- [24] B. Armitage, C. J. Yu, C. Devadoss, G. B. Schuster, *J. Am. Chem. Soc.* **1994**, *116*, 9847–9859.
- [25] J. B. Chaires, M. J. Waring, *Drug–Nucleic Acid Interactions*, Vol. 340, Academic Press, San Diego, 2001.
- [26] E. C. Long, J. K. Barton, *Acc. Chem. Res.* **1990**, *23*, 271–273.
- [27] B. Norden, T. Kurucsev, *J. Mol. Recognit.* **1994**, *7*, 141–155.
- [28] B. Norden, M. Kubista, T. Kurucsev, *Q. Rev. Biophys.* **1992**, *25*, 51–170.
- [29] G. B. Schuster, *Acc. Chem. Res.* **2000**, *33*, 253–260.
- [30] S. M. Gasper, B. Armitage, X. Q. Shui, G. G. Hu, C. J. Yu, G. B. Schuster, L. D. Williams, *J. Am. Chem. Soc.* **1998**, *120*, 12402–12409.
- [31] E. Schlittler, J. Hohl, *Helv. Chim. Acta* **1952**, *35*, 29–45.
- [32] H. Ihmels, K. Faulhaber, C. Sturm, G. Bringmann, K. Messer, N. Gabellini, D. Vedaldi, G. Viola, *Photochem. Photobiol.* **2001**, *74*, 505–511.
- [33] G. Viola, F. Dall'Acqua, N. Gabellini, S. Moro, D. Vedaldi, H. Ihmels, *Chem-BioChem* **2002**, *3*, 550–558.
- [34] R. Alberto, R. Schibli, A. Egli, P. A. Schubiger, W. A. Herrmann, G. Artus, U. Abram, T. A. Kaden, *J. Organomet. Chem.* **1995**, *493*, 119–127.
- [35] R. Alberto, A. Egli, U. Abram, K. Hegetschweiler, V. Gramlich, P. A. Schubiger, *J. Chem. Soc. Dalton Trans* **1994**, 2815–2820.

Received: June 22, 2004

Published online: January 13, 2005